SI Materials and Methods: Simulations to test methodology

We use raw observed abundance in open communities to calculate the strength of negative frequency dependence (NFD) for all persistent species. The wide availability of abundance data makes the generality of our conclusions possible, but it also creates uncertainty in our estimates. Density dependence is typically overestimated in the presence of observation uncertainty (1–3). The same bias could also influence our estimates of frequency dependence. Another source of measurement error is immigration and emigration. Assuming a species experiences net immigration in a low abundance year (relative to surrounding locations), and net emigration in a high abundance year, the estimate of density dependence will be inflated for that species. This tendency to detect density dependence in abundance data even when none exists means that we cannot obtain reliable estimates of NFD without correcting for this bias somehow.

We are not, however, interested in the precise estimates of NFD for each species in each community so much as we are interested in the pattern created when rare species have disproportionately strong NFD relative to their common counterparts. Focusing on the relative strength of NFD removes the need for unbiased estimates of population model parameters for every species in the community (1). There are, however, further sources of bias that may still contaminate our estimate of the overall pattern of asymmetric NFD. For example, the rare species in our abundance estimates might be prone to greater measurement error than the common species, leading to the asymmetric NFD pattern. Measurement error is not the only, or even most likely, potential source of bias when estimating NFD from abundance data. There are also potential artifacts related to the relationship between the slope and x-intercept, as well as possible direct or indirect effects of the number of species. We use randomizations of the raw abundance data to control for all these potential sources of bias simultaneously.

To demonstrate the effectiveness of our methods for controlling for different sources of bias, we simulated species abundances with known NFD and used our methodology to quantify the relationship between equilibrium frequency and NFD. In each simulation, population growth depended on negative frequency dependence and demographic stochasticity as follows:

$$n_{s,t+1} = \exp(FD_s * N_{s,t}/C_t + IGR_s) * N_{s,t}$$

$$N_{s,t+1} \sim \text{Pois}(n_{s,t+1})$$

Where $n_{s,t+1}$ is the expected abundance of species *s* in time *t+1* and C_t is the total community abundance in time *t*. *IGR* represents the intrinsic growth rate and *FD* represents the frequency dependence experienced by each species *s*. $N_{s,t+1}$ is the true abundance of species *s* in time *t+1*, after incorporating demographic stochasticity with a Poisson distribution.

We then incorporated measurement error by drawing observed abundances, X, from a negative binomial distribution with mean $N_{s,t+1}$ and dispersion parameter *k*:

$$X_{s,t+1} \sim NB(N_{s,t+1}, k)$$

All simulations were initialized with a total community abundance of 1000 individuals. We used the values in Table S2 to represent multiple possible scenarios for the empirical relationship between NFD and equilibrium frequency (Figure S1). Scenario 1 represents communities with no relationship between equilibrium frequency and NFD. Scenario 2 represents communities with a weak relationship between equilibrium frequency and NFD. Note that in this community, rare species experience smaller maximal growth rates than common species. Scenario 3 represents a moderate relationship between equilibrium frequency and NFD, and one in which all species are experiencing similar maximal growth rates (1, in this case). Scenario 4 represents communities with a strong relationship between equilibrium frequency and NFD. In these scenarios, rare species will often experience larger maximal growth rates than common species, in addition to steeper NFD. In each of these scenarios, the equilibrium frequencies *f* of the 10 species remain constant. Only the strength of NFD changes, and the relationship between equilibrium frequency and NFD as a result, but basic community structure is unaltered (Figure S2).

We altered the relationship between the values of the dispersion parameter and the equilibrium frequency to demonstrate the robustness of our methodology to biases in sampling. We examined three different models for how sampling bias could influence our results (Figure S3). First we examined whether sampling noise affecting all species equally influenced our ability to detect the pattern of interest (Table S2, sampling model A, k=1). The remaining two sampling models also demonstrate the robustness of our methods to sampling noise that is based on species abundance. Setting the dispersion parameter k equal to $10*f$ simulates sampling in which uncertainty, in the form of clustering, is higher for rare species (Table S2, sampling model B, $k=10*f$). Setting the dispersion parameter k equal to $0.1/f$ simulates sampling in which uncertainty, in the form of clustering, is higher for more common species (Table S2, sampling model C, $k=0.1/f$). This final scenario is not based on a known potential bias, but is included to thoroughly demonstrate the robustness of the model.

For the data generated from each of these simulations, we assessed whether our randomization technique (see Methods, main text) could distinguish between real patterns in the underlying community from patterns that may have been generated by various sources of bias. The simulation results demonstrate the ability of our bias control methods to detect and remove relationships between equilibrium frequency and NFD created entirely by artifacts (the uncertainty bias, mean/variance ratios resulting from sampling bias, etc.). The benefit of this general method relying on randomizations is its generality. It is not necessary to know what sources of bias may plague each community in our analysis. The randomizations detect any pattern in the data that may create the asymmetric NFD pattern, other than one related to

frequency dependence in the time series (Figures S4 – S7). Thus, we are able to treat all communities uniformly.

The randomizations do not, however, account for uncertainty in the individual estimates of negative frequency dependence. By treating all communities uniformly, we do not incorporate time lags, cycles, or nonlinearities, among other possibilities, though in certain communities it would likely be appropriate. Though the randomization does account for some of the effects of emigration and immigration, there is one bias specifically we are unable to account for, because we are unable to differentiate *in situ* population growth from immigration. If rare species are more likely to be net population sinks than common species in the observed sample, this could create asymmetric NFD. It is extremely unlikely that this produces the pattern we see in every single community, but does mean that we cannot rule it out as a possibility for an individual community. As a result, we do not make conclusions based on any individual species, but the prevalence of asymmetric NFD over all communities. We leave improved estimates of these individual parameters to further research.

The simulation results also support the assertion that our method is very conservative, and is not able to detect real negative equilibrium frequency-NFD relationships when the pattern is weak (Figures S5 – S6). Therefore, we are unable to distinguish between a pattern created entirely by bias, and one that is weak, but real. On the other hand, when our method does detect a significant association between equilibrium frequency and NFD, we can be confident that the relationship is not only present, but very strong. Again, we leave the detection of weakly asymmetric NFD in some of these specific communities to future, more targeted, research.

References

1. Knape J, de Valpine P (2012) Are patterns of density dependence in the Global Population Dynamics Database driven by uncertainty about population abundance? *Ecol Lett* 15:17–23.

2. Dennis B, Ponciano JM, Lele SR, Taper ML, Staples DF (2006) ESTIMATING DENSITY DEPENDENCE, PROCESS NOISE, AND OBSERVATION ERROR. *Ecol Monogr* 76:323–341.

3. Herrando-Pérez S, Delean S, Brook BW, Bradshaw CJA (2012) Density dependence: an ecological Tower of Babel. *Oecologia* 170:585–603.

Table S2. Summary of the parameter values used in our simulations. All combinations of the NFD scenarios and sampling values were run.

Species	Equilibrium frequency (*f*)	NFD Scenario 1		NFD Scenario 2		NFD Scenario 3		NFD Scenario 4		Sampling model (*k* values)		
		IGR	*FD*	*IGR*	*FD*	*IGR*	*FD*	*IGR*	*FD*	A: Constant	B: 10* *f*	C: 0.1/*f*
1	0.001	0.001	-1	0.032	-31.62	1	-1000	31.62	-31622.78	1	0.01	100
2	0.01	0.01	-1	0.100	-10.00	1	-100	10.00	-1000	1	0.1	10
3	0.02	0.02	-1	0.141	-7.07	1	-50	7.07	-353.55	1	0.2	5
4	0.04	0.04	-1	0.200	-5.00	1	-25	5.00	-125	1	0.4	2.5
5	0.08	0.08	-1	0.283	-3.54	1	-12.5	3.54	-44.19	1	0.8	1.25
6	0.09	0.09	-1	0.300	-3.33	1	-11.11	3.33	-37.04	1	0.9	1.1
7	0.149	0.149	-1	0.386	-2.59	1	-6.71	2.59	-17.39	1	1.49	0.67
8	0.16	0.16	-1	0.400	-2.50	1	-6.25	2.50	-15.63	1	1.6	0.63
9	0.18	0.18	-1	0.424	-2.36	1	-5.56	2.36	-13.09	1	1.8	0.56
10	0.27	0.27	-1	0.520	-1.92	1	-3.70	1.92	-7.13	1	2.7	0.37

Figure Legends

Figure S1: The frequency-dependence relationships simulated in each community scenario. In each case, the species' equilibrium frequencies are the same (see model above). Only the strength of NFD experienced by each species (steepness of the line) is changed in each scenario, to create differing strengths of the equilibrium frequency-NFD relationship ('pattern').

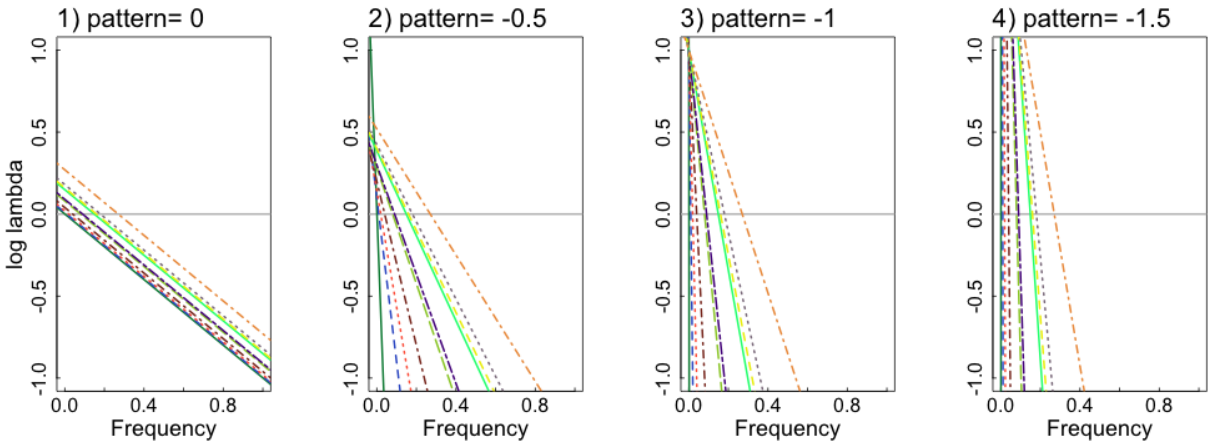

Figure S2: The resulting actual species abundances in simulated community scenarios 1 (panel 1), 2 (panel 2), 3 (panel 3), and 4 (panel 4).

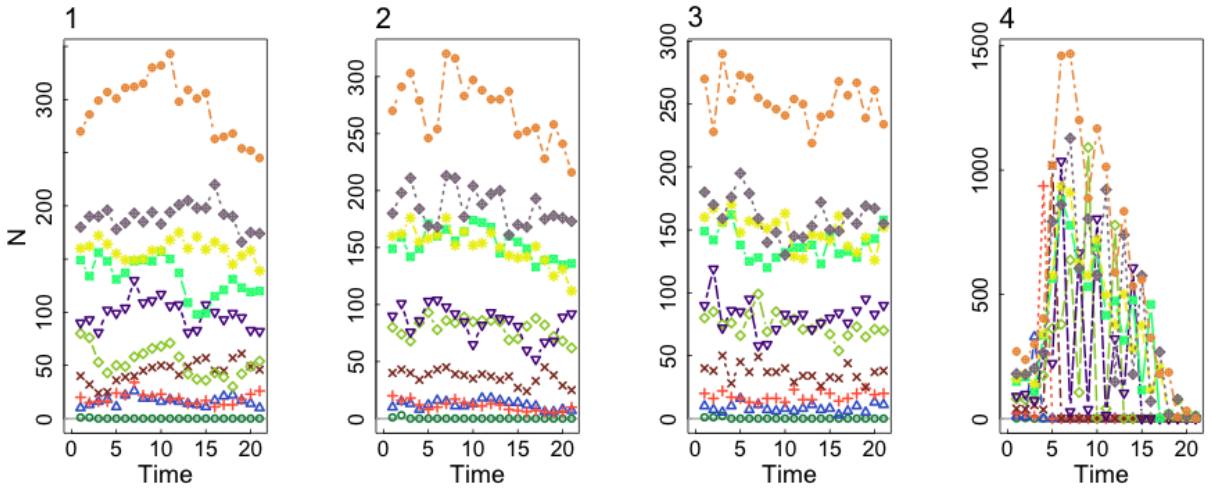

Figure S3: The resulting observed species abundances in the nine simulated communities, after incorporating sampling noise. Each column of figures displays the data from one NFD scenario; scenario 1 (panel 1), 2 (panel 2), 3 (panel 3), or 4 (panel 4). Each row of figures displays the data from one set of sampling bias values; Constant dispersion parameter (*k*=1, row A); dispersion parameter decreases with rarity (*k*=10**f*); or dispersion parameter increases with rarity (*k*=0.1/*f*).

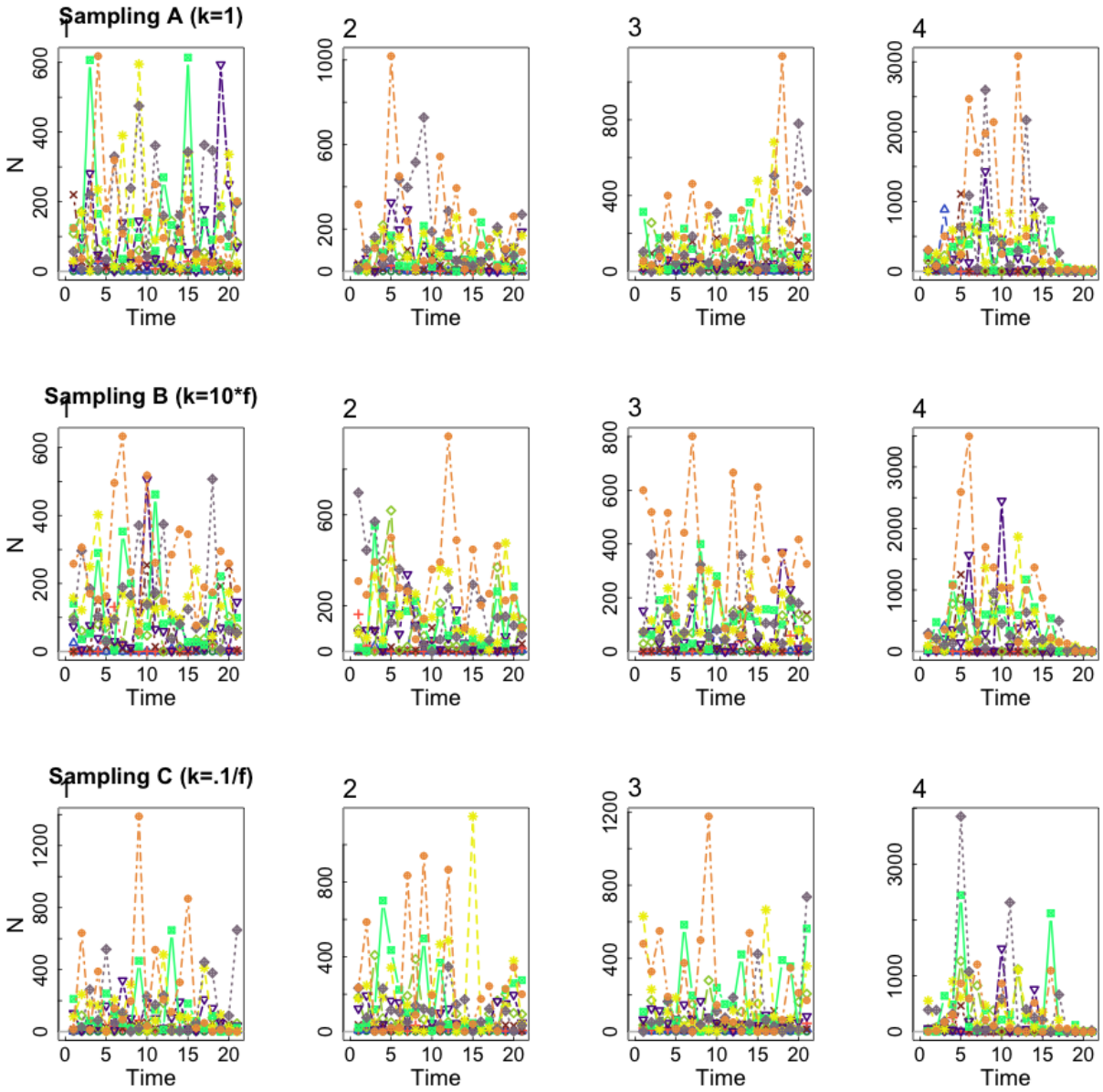

Figure S4: Results of simulation of Scenario 1, using the same methodology applied to the real community data. The first figure in each panel shows the calculated relative abundances and growth rates from the simulated data for 10 species (points). Lines represent the estimated relationship for each species. The second figure shows the relationship between equilibrium frequency and the strength of NFD in each simulated community (red lines are the fitted log-log relationship). The third figure shows histograms of the 'Null' pattern estimated from the shuffled data in 5000 randomizations. The vertical red line is the pattern estimated from the simulated data for comparison. This is how p values were calculated (for use in false discovery rate control). The dispersion parameter was constant (A, k=1), increased with rarity (B, k=10*f), or decreased with rarity (C, k=0.1/f). In this scenario with no relationship between equilibrium frequency and NFD, the randomization methods correctly detect no significant relationship.

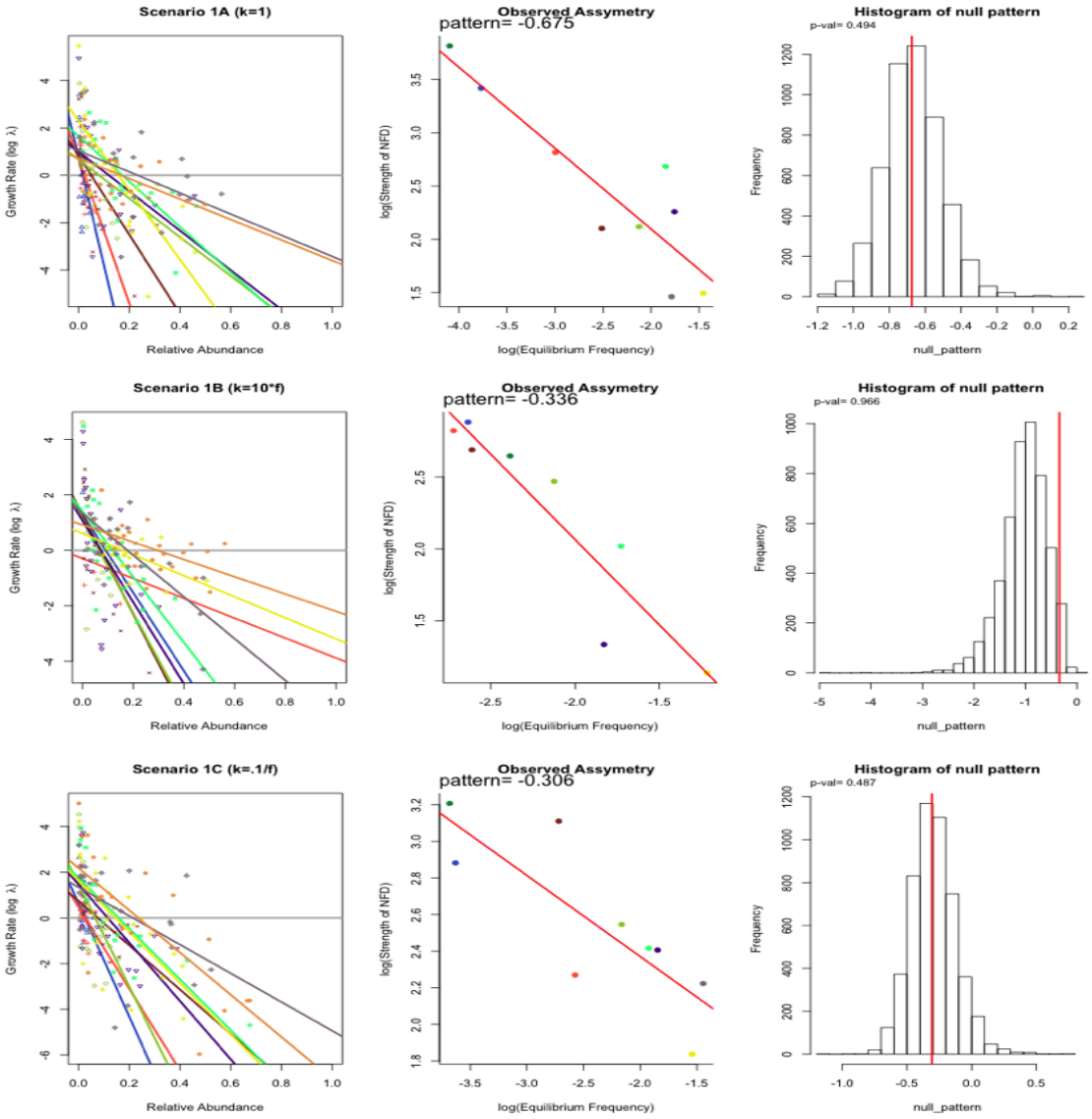

142

143

144

145

146

147

Figure S5: Results of simulation of Scenario 2, using the same methodology applied to the real community data. The first figure in each panel shows the calculated relative abundances and growth rates from the simulated data for 10 species (points). Lines represent the estimated relationship for each species. The second figure shows the relationship between equilibrium frequency and the strength of NFD in each simulated community (red lines are the fitted log-log relationship). The third figure shows histograms of the 'Null' pattern estimated from the shuffled data in 5000 randomizations. The vertical red line is the pattern estimated from the simulated data for comparison. This is how p values were calculated (for use in false discovery rate control). The dispersion parameter was constant (A, k=1), increased with rarity (B, k=10*f), or decreased with rarity (C, k=0.1/f). In this scenario with a weak relationship between equilibrium frequency and NFD, the randomization methods cannot distinguish between an artificial relationship created by uncertainty in the observations and the real pattern.

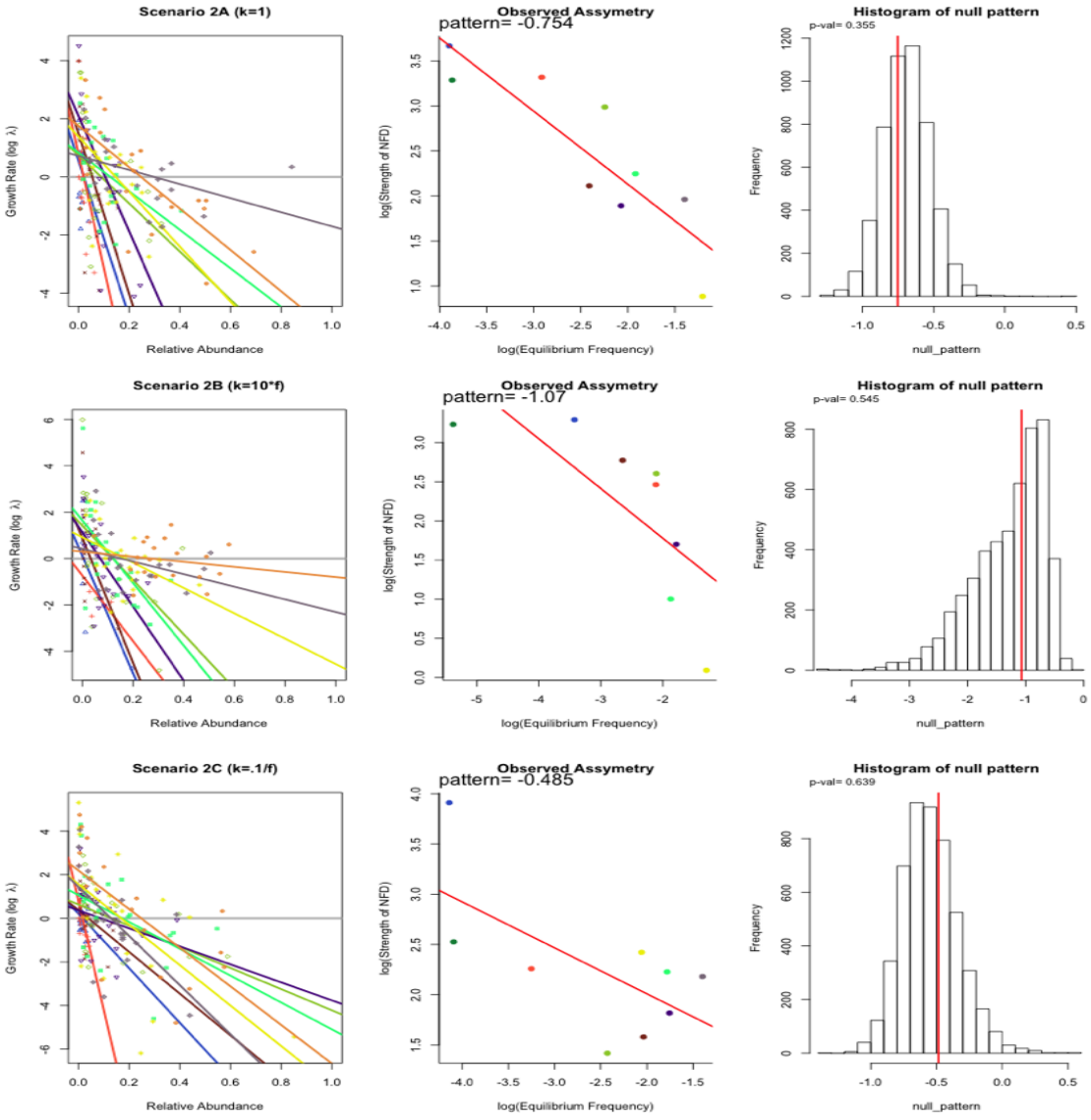

159

160

161

162

163

164

Figure S6: Results of simulation of Scenario 3, using the same methodology applied to the real community data. The first figure in each panel shows the calculated relative abundances and growth rates from the simulated data for 10 species (points). Lines represent the estimated relationship for each species. The second figure shows the relationship between equilibrium frequency and the strength of NFD in each simulated community (red lines are the fitted log-log relationship). The third figure shows histograms of the 'Null' pattern estimated from the shuffled data in 5000 randomizations. The vertical red line is the pattern estimated from the simulated data for comparison. This is how p values were calculated (for use in false discovery rate control). The dispersion parameter was constant (A, k=1), increased with rarity (B, k=10*f), or decreased with rarity (C, k=0.1/f). In this scenario with a moderate relationship between equilibrium frequency and NFD, the randomization methods cannot distinguish between an artificial relationship created by uncertainty in the observations and the real pattern.

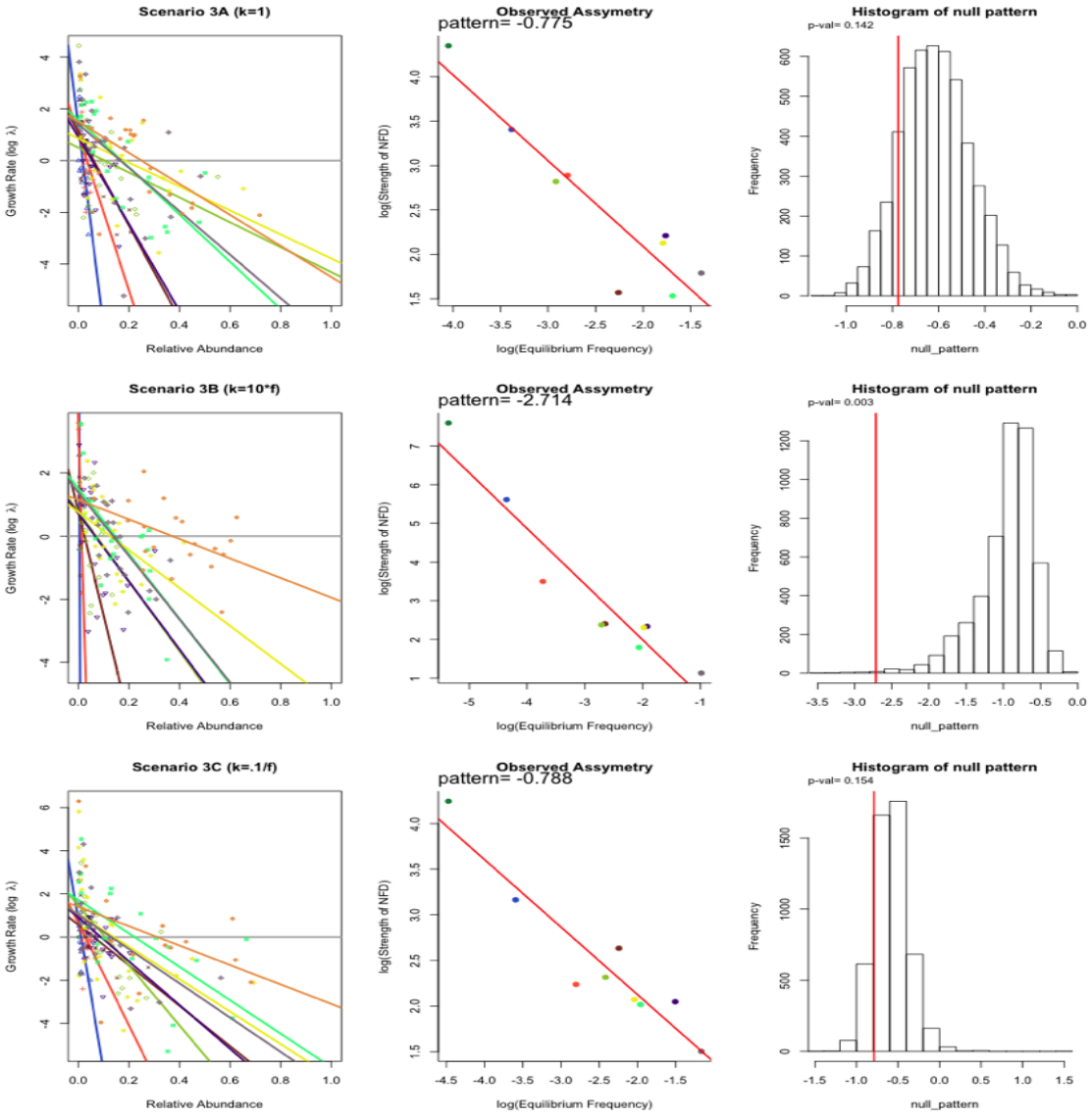

176

177

178

179

180

181

Figure S7: Results of simulation of Scenario 4, using the same methodology applied to the real community data. The first figure in each panel shows the calculated relative abundances and growth rates from the simulated data for 10 species (points). Lines represent the estimated relationship for each species. The second figure shows the relationship between equilibrium frequency and the strength of NFD in each simulated community (red lines are the fitted log-log relationship). The third figure shows histograms of the 'Null' pattern estimated from the shuffled data in 5000 randomizations. The vertical red line is the pattern estimated from the simulated data for comparison. This is how p values were calculated (for use in false discovery rate control). The dispersion parameter was constant (A, k=1), increased with rarity (B, k=10*f), or decreased with rarity (C, k=0.1/f). In this scenario with a strong relationship between equilibrium frequency and NFD, the randomization methods correctly detect a significant pattern, while accounting for the biased pattern created from observation uncertainty.

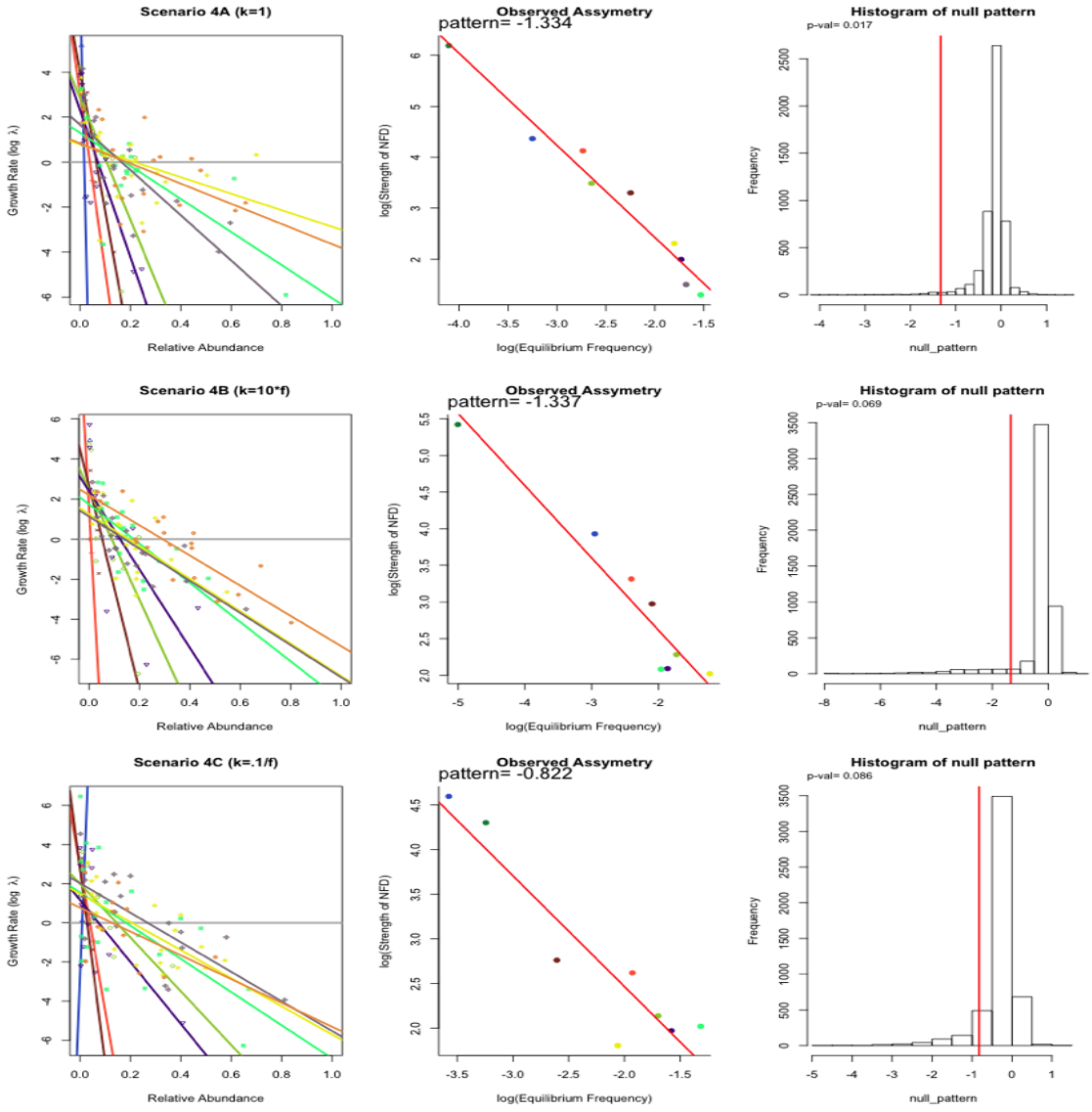
Scenario 4A (k=1)
Growth Rate (log λ)
Relative Abundance
Observed Assymetry
pattern= -1.334
log(Strength of NFD)
log(Equilibrium Frequency)
Histogram of null pattern
p-val= 0.017
Frequency
null_pattern
Scenario 4B (k=10*f)
Growth Rate (log λ)
Relative Abundance
Observed Assymetry
pattern= -1.337
log(Strength of NFD)
log(Equilibrium Frequency)
Histogram of null pattern
p-val= 0.069
Frequency
null_pattern
Scenario 4C (k=.1/f)
Growth Rate (log λ)
Relative Abundance
Observed Assymetry
pattern= -0.822
log(Strength of NFD)
log(Equilibrium Frequency)
Histogram of null pattern
p-val= 0.086
Frequency
null_pattern

194